

Chapter 3

Scale-up of Sonochemical Reactors for Water Treatment

(Reproduced in part with permission from *Industrial and Engineering Chemistry Research*, **2001**, 40, 3855-3860. Copyright 2001 American Chemical Society)

Abstract

A novel pilot-plant scale sonochemical reactor (UES 4000 C Pilotstation) has been specifically developed for degrading a variety of water contaminants in large-scale applications. We report here the sonochemical degradation of four chemical compounds in aqueous solution: the chlorinated volatile contaminants dichloromethane (DCM) and trichloroethylene (TCE), and two non-volatile compounds, phenol and the azo dye methyl orange (MO). The flow-through reactor in the Pilotstation consists of four 612 kHz piezoelectric transducers which are driven by a power source operating at 3 kW. The sonochemical reaction chamber has a volume of 6 L, while the total capacity of the Pilotstation, including a heat-exchanger unit and a reservoir tank varies from a minimum volume of 7.25 L to a maximum over 45 L. The observed reaction rates for the degradation of these contaminants in the Pilotstation were compared with values determined under similar conditions in small-scale bench reactors in order to evaluate its performance over a wide range of power densities. The pseudo-first order degradation rate for TCE in the Pilotstation was found to be more than 4 times higher than corresponding smaller values measured in lab-scale reactors. Furthermore, the observed rates for DCM degradation also exceeded those of the small-scale reactors by factors from 3 to 7. The degradation rate of these two chlorinated compounds was faster with decreasing initial concentration, in all cases. Experiments with 10 μM MO (aq) in the Pilotstation operating at different total volumes exhibited a linear dependence between the observed rate constants for sonolysis and the applied power density (PD), in the range $67 < \text{PD (W/L)} < 414$. Initial sonochemical degradation rates for phenol were modeled with zero-order kinetics, requiring that all rate constants be normalized with respect to

concentration for comparison between the Pilotstation and the lab-scale reactors. As with the chlorinated hydrocarbons, phenol degradation was found to be 2-5 times faster in the UES-4000C reactor, and normalized degradation rates increased with decreased initial concentrations. Steady-state $\cdot\text{OH}$ (aq) radical concentrations in each reactor were calculated, and were shown to correlate with the applied power density in the vessel. A power budget analysis was done for the Pilotstation, which indicates that nearly one third of the applied power is converted in sonochemical activity. Comparisons of power density utilization between sonochemical methods and photocatalytic techniques applied to the same chemical systems show an important improvement (up to two orders of magnitude) of efficiency when ultrasonic irradiation is employed. This fact illustrates the potential of sonochemistry as a useful advanced oxidation process.

Introduction

Ultrasonic irradiation is employed in a variety of industrial processes, such as welding of thermoplastics, and metals, homogenization of emulsions, dispersion of paints, cleaning and degreasing.^{1,2} However, sonochemistry (i.e., chemical reactions produced by sonication of liquids) has not yet received much attention as an alternative for large-scale chemical processes. Chemical reactions are induced upon high-intensity acoustic irradiation of liquids at frequencies that produce cavitation (in the range 20 – 1000 kHz). Solvent molecules and volatile solute molecules, which constitute the gaseous phase inside those cavities, are subject to extreme conditions upon bubble collapse.¹⁻³ Primary thermal reactions inside the cavitating bubble as well as solution radical chemistry are the two main pathways of sonochemistry. Sonochemical methods are potentially suitable for a variety of industrial applications, since chemical reactions can be produced by relatively simple piezoelectrical devices in a controlled regime, without addition of reagents. The fact that extreme temperatures (in the order of thousands of K) are reached in localized hot-spots in the liquid while the bulk fluid remains at low (i.e., room) temperature and pressure, facilitates reactor design and makes sonochemistry a very versatile technique. However, only a few examples of the application of sonochemistry for large-scale chemical synthesis have been reported.⁴⁻⁶

Water treatment technologies must be continuously upgraded, particularly in the field of advanced oxidation processes (AOPs), in order to meet the more demanding water quality standards for groundwater decontamination and industrial wastewater discharge. The sonochemical degradation of a variety of water contaminants (chlorinated and aromatic hydrocarbons, dyes, surfactants, pesticides, herbicides) has been

successfully proven in bench-scale experiments. In addition, kinetic and mechanistic aspects of these reactions have been elucidated (*vide infra*). Ultrasonic frequencies in the range 100-1000 kHz have been shown to be more practical than lower frequencies around 20 kHz.⁷⁻¹⁰ At higher frequencies, cavitation is produced in the liquid phase far from the surface of the transducer, thus protecting it from the mechanical erosion generated by bubble implosion. Transducers, which operate at 20 kHz, must be periodically replaced due to this problem.² The present challenge is to scale-up sonochemical processes in order to meet industrial needs in terms of volumetric flow rates, reaction energy rates, efficiencies and overall costs. In this paper, we present a pilot-plant reactor system (Pilotstation), which is able to sonochemically process up to 45 L of solution operating at 3 kW. This constitutes a 20-fold and 30-fold increase respectively, as compared with typical bench-scale reactor volumes and applied powers. Evaluation of sonochemical efficiency for several different reactions, as well as intrinsic problems related to the scale-up of the reactors (e.g., heat dissipation), is addressed.

Sonochemical Degradation of Chemical Contaminants in Water

In recent years there have been a growing number of reports pertaining to the degradation of organic pollutants in water using high-frequency, high-power sonolysis.¹¹⁻²³ Volatile chlorinated hydrocarbons are particularly well suited to sonochemical degradation, since they are readily concentrated within the vapor phase of the cavitation bubbles where they react readily through thermolytical cleavage of C-Cl bonds at relatively low temperatures during cavitation bubble collapse.^{11,18} The reaction rate for the depletion of these molecules typically increases with the liquid temperature in

proportion to their intrinsic vapor pressures, which indicates the predominance of high-temperature gas phase pyrolysis reactions.¹⁸ Since chlorinated methanes are not very susceptible to reaction with most oxidants in aqueous solution, sonolysis appears to be a convenient alternative to standard oxidative techniques. In this study, we used dichloromethane (DCM, CH_2Cl_2) and trichloroethylene (TCE, C_2HCl_3) as probes for volatile sonochemical targets.

Non-volatile substrates are also subject to sonochemical degradation. In this case, the process is mediated by active species generated in the thermolysis of solvent molecules inside the cavitation bubbles, particularly $\cdot\text{OH}$ (aq), $\cdot\text{HO}_2$ (aq) and $\cdot\text{O}_2^-$ (aq) radicals and H_2O_2 (aq).^{2,7,17,24} Each cavitation event generates a burst of these active species into solution, where they participate in low-temperature oxidation processes involving the target molecules. The production rate of active species by cavitation events increases with decreasing temperature, because an excess vapor pressure inside the bubble cushions the cavitation bubble collapse, thus reducing drastically the final temperature reached upon implosion.²⁵⁻³² For this reason, sonolysis rates of non-volatile compounds decrease with increasing temperature, which is the opposite effect that is observed with volatile solutes. In order to address this particular situation, we have studied phenol ($\text{C}_6\text{H}_5\text{OH}$) and the anionic azo dye methyl orange (MO, $\text{C}_{14}\text{H}_{14}\text{N}_3\text{NaO}_3\text{S}$) as probes for non-volatile solutes that preferentially reacts with $\cdot\text{OH}$ radicals, in an effort to compare the Pilotstation performance with our previous results obtained with small-scale reactors.^{16,17}

Experimental setup

The UES 4000-C Pilotstation employed in this study is the first pilot-plant prototype of its kind reported for water treatment. Figure 1 illustrates schematically our experimental setup. It consists on a 6 L stainless steel flow vessel containing four 612 kHz piezoelectrical transducers attached to it. Each transducer is excited by a tunable generator, which operates at a maximum power of 4 kW (1 kW per transducer). The present experiments were performed operating at 75 % of full capacity, i.e., 3 kW total applied power. The transducer surfaces are individually cooled by circulation of chilled water on their internal surfaces, by means of a 1.5 kW thermostat (VWR 1157). A thin 0.1 mm Polytrifluoroethylene (PTFE, Teflon ®) window parallel to each transducer separates the solution under irradiation from the chilled water. The four acoustic windows are located between each cooling jacket (9) and the vessel (1), allowing the sound waves to reach the solution (Figure 2).

To dissipate the heat that results from the sonolysis of water, a peristaltic pump (Masterflex 7591-50) circulated the solution under treatment from the vessel to a heat exchanger unit (Sentry WSW 8222, 0.5 L). The pump accommodates flow velocities ranging from 1.5 to 12 L/min and the flow loop can be easily adapted from this semi-batch mode to a continuous flow configuration simply by connecting the reservoir tank on-line at the outlet of a process discharge. A 1.8 kW chiller (VWR 1176) was used to circulate a water/alcohol refrigerant mixture through the heat exchanger in order to control the temperature of operation of the solution under test.

When operated at its minimum volume (i.e., 7.25 L) relatively large spatial and temporal temperature gradients are established within the Pilotstation reactor. Figures 3

and 4 illustrate the temperature profiles at four flow rates ($F = 1.5, 4, 9, 12$ L/min) for pure water exiting the heat exchanger (T_1) and the ultrasonic vessel (T_2), respectively. These profiles illustrate that while the median temperature within the ultrasound reactor does not change appreciably with changes in the flow rate, the disparity in temperatures between the entrance and exit points increases significantly for $F \leq 4$ L/min. (Fig. 5) To more effectively compare the performance of the large reactor to smaller isothermally operated bench-scale units, an operational rate of 6 L/min was chosen. This flow rate achieved the highest mean hydrodynamic residence time while maintaining a quasi-isothermal environment within the reactor. Figure 6 shows the temperature profiles obtained at 6 L/min, starting at 2 °C. By adding ice to the thermostat, the median temperatures within were further stabilized within the first five minutes in the range $T_1 = 8-9$ °C, $T_2 = 12-13$ °C, and $T_3 = 4-5$ °C during the duration of the experiment.

A controlled pressure of background gas (such as Ar or O₃/O₂ mixtures) can be used to saturate the solution entering the heat exchanger. The vessel and the heat exchanger operate at ambient pressure in an open system configuration, thus experiments can be run under air saturation, without further gas spurge. We have tested the system for possible evaporative losses of volatile substrates during the runs. In the present operation conditions (i.e., low temperature and short run times) these represent less than 2-4 % of the initial DCM concentration.

The observed reaction rates were compared with previous and new experiments at 15 °C performed in two bench-scale sonochemical reactors (Allied Signal-ELAC Nautik USW and Undatim, $V = 0.60$ and 0.65 L, respectively). The ELAC reactor employs a bottom-mounted 358 kHz transducer operated at 100 Watts while the Undatim reactor is

a side-mounted 500 kHz reactor which operates at 50 Watts. Both reactors are glass vessels with integrated water jackets for cooling. All runs were performed at 15 °C and were maintained at this temperature with a 1.5 kW thermostat (VWR 1157). The emitting area of the ELAC transducer is 23.6 cm² while the Undatim transducer is 25 cm². Although the frequencies of these lab-scale reactors are lower than that of the Pilostation (612 kHz), frequency effects on the measured rates are optimal in this range.^{10,12,33} The reported applied power for the small reactors has been previously determined using standard calorimetric procedures.¹²

Aliquots (1 mL) were taken as a function of time and analyzed to quantify the concentrations of the substrates. TCE and DCM were quantified chromatographically with a Hewlett Packard 1090 Series II HPLC monitored with UV detection, equipped with a ODS Hypersil 5 µm, 100 x 2.1 mm column at 40 °C, and eluted with a mixture of 70/30 and 50/50 methanol/water, respectively. Additionally, DCM was quantified with a Hewlett Packard 5890 Series II Plus GC with a headspace sampler and ECD detection. The headspace sampler heated the sealed vials to 70 °C for 10 min before transferring the headspace gasses to a HP-5, 30 m x 0.32 mm x 0.25 µm (film thickness) column at 52 °C. An inlet temperature of 170 °C and a detection temperature of 270 °C were used. Phenol was quantified with the same HPLC instrument mentioned previously equipped with a Restek Pinnacle IBD 5 µm, 250 x 3.2 mm column at 40 °C and an elution mixture of 40/60 methanol/water. MO was quantified by UV-vis spectroscopy at $\lambda = 464$ nm with a Hewlett Packard 8452A diode-array spectrophotometer.

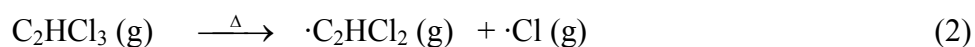
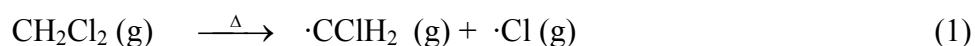
MO (Baker, >95 %), TCE (Aldrich, >99 %), DCM (EM Science, >99 %) and phenol (EM Science, >99%) were used without further purification. The solutions were

prepared with water purified by a Millipore Milli-Q UV Plus system ($R = 18.2 \text{ M}\Omega \text{ cm}$). The solutions were not buffered or adjusted for pH.

Results and Discussion

Kinetics of sonochemical reactions

All four studied substrates degraded quasi-exponentially in the Pilotstation reactor. This is in agreement with previous experience in small reactors for these systems, where the primary degradation step in each case was described as^{11,16,18,34}



Reactions 1 and 2 take place in the gas phase inside the cavitation bubbles, while reactions 3 and 4 occur in solution. The degradation profiles for DCM, TCE and MO were fit to pseudo first-order kinetics over at least three half-lives.

$$-\left(\frac{d[X]}{dt}\right)_{US} = {}^{US}k_{-X}[X] \quad (5)$$

where X = DCM, TCE, or MO.

While phenol was found to degrade with apparent first-order degradation kinetics as well, these experiments were limited by reactor duty cycles ($\tau < 30 \text{ min}$) and experimental profiles were typically measured for only 1 half-life. Therefore, initial

degradation rates are reported for this compound. Initial concentration vs. time profiles were fit to a normalized zero-order rate constant, k'_{-ph} .

$$\frac{[C_6H_5OH]}{[C_6H_5OH]_o} = 1 - \left(\frac{k_{-ph}}{[C_6H_5OH]_o} \right) t = 1 - (k'_{-ph})t \quad (6)$$

Trichlorethylene (TCE) and Dichloromethane (DCM) Degradation

Table 1 summarizes the observed pseudo first-order rate constants, k_X , measured under the given experimental conditions for X = DCM and TCE with air saturation (i.e., without additional gas sparging), working both with the Pilotstation (Flow = 6 L/min, Volume = 7.25 L) and with bench-scale reactors. The values for the chlorinated volatile substrates are plotted in Figure 7. For both substrates, we observed an important concentration effect, with sonolysis rates decreasing with increasing initial concentration. The competition with intermediates and byproducts can be accounted for this variation of the rate of substrate depletion. Independent of the type of reactor employed, TCE sonolysis was always faster than that of DCM. This can be explained by the higher value of the Henry's law constant for TCE ($H_{TCE} = 1.03 \text{ kPa m}^3 \text{ mol}^{-1}$) than for DCM ($H_{DCM} = 0.30 \text{ kPa m}^3 \text{ mol}^{-1}$).³⁵ Sonolysis rate constants were shown³⁶ to increase with H_X for chlorinated methanes, ethanes and ethenes in the range of $0.09 \leq H_X \text{ (kPa m}^3 \text{ mol}^{-1}) \leq 2.45$ as $k_X \cong H_X^{0.30}$. Over the range of power densities, the degradation rates of both substrates increased linearly, although the DCM data seemed to have enhanced performance with the Pilotstation operating at 414 W/L than what would be expected from a linear extrapolation of the bench-top reactor data for this compound. According with the calculated half-life times for TCE and DCM in the Pilotstation, 90 % degradation

is achieved in only 11 min and 17-25 min, respectively. Considering that the entire reactor setup consumes ~ 7 kW (including the two thermostats, the transducers and the pump), the cost of eliminating 90 % of those contaminants would range between 0.15 to 0.40 kWh/L. A similar calculation for the small reactors results in a level of power usage (0.08 to 0.21 kWh/L) that is comparable, if the calculation is based exclusively on the power of the transducers (50 W). The use of a 1 kW thermostat in bench-reactors setup increases that cost to values in the range 1 to 4 kWh/L. Furthermore, these energy cost evaluations can be compared favorably with other advanced oxidation technologies. Choi and Hoffmann required a much higher power density (26 kWh/L) to achieve similar rates in the photodegradation of halomethanes in aqueous TiO_2 suspensions.³⁷

Methyl Orange (MO) Degradation

Figure 8 illustrates the experiments performed with different total reactor volumes for 10 μM MO solutions (ranging from $V = 7.25$ to 45 L), together with values from two small reactors (0.6 L and 0.65 L, respectively). The bench-scale reactors were run in the batch mode, except for one case in which the reactor was operated in continuous flow with an external reservoir tank (total volume 2 L) in order to evaluate its scale-up efficiency. In the case of the Pilotstation, we observed a linear correlation of the observed pseudo first-order rate constants (k_{MO}) with the applied power density (PD) over the entire power density range:

$$k_{\text{MO}} (\text{min}^{-1}) = 2.06 \times 10^{-4} [\text{PD} (\text{W L}^{-1})] + 7.4 \times 10^{-5} \quad (7)$$

The degradation of MO as determined by its loss of color has been shown a good probe to account for $\cdot\text{OH}$ radical production in sonochemistry.^{16,17} The fact that the

observed sonochemical activity is not hindered or saturated up to 450 W/L is promising, and suggests that even more compact vessels could be built, or a higher power density could be used. Under Ar saturation, MO bleaching was found to be 9.6 % faster ($k_{\text{MO}}^{\text{Ar}} = 0.097 \text{ min}^{-1}$ for $V = 7.25 \text{ L}$, not included in Figure 5), which is in good agreement with the rate increments observed for the same reaction at the bench scale.¹⁶ A cost estimation for 90 % degradation of MO in the Pilotstation under air saturation, which is achieved in an average of 3.8 min/L, would be 0.44 kWh/L.

Pseudo first-order rate constants of MO bleaching in one of the bench-scale reactors (Allied Signal), operating at 100 W in batch and flow configurations, fall below the values reported with the Pilotstation in Figure 5. The other small reactor (Undatim) had a better performance under similar experimental conditions, exhibiting higher reaction rates than the Pilotstation operating at similar power densities (see Table 1). These very different performance characteristics observed for the different reactors can be attributed most likely to effects related with the reactor geometries and configurations. Processes of propagation and absorption of the acoustic field inside the different vessels are a factor that may affect strongly the reactor performance. This aspect of sonochemistry has not been properly addressed to date, and should be the subject of more systematic study in the future.

Phenol Degradation

Table 2 summarizes the observed initial degradation rate constant values, $k'_{\text{-Ph}}$, in both the lab-scale and in the Pilotstation reactor. The relatively low vapor pressure and Henry's constant of phenol³⁸, $4.7 \times 10^{-2} \text{ kPa}$ and $4.0 \times 10^{-5} \text{ kPa m}^3 \text{ mol}^{-1}$, respectively,

preclude significant pyrolysis of this compound within acoustic cavitation bubbles. The mechanism of sonolytic phenol degradation is, therefore, limited to free-radical attack in the solution. Initial rate constants achieved in the Pilotscale reactor were found to be 2-5 times larger as compared to the observed rates in the Allied Signal bench-scale unit. This enhancement scales well with the power density ratio of 2.5 between the two systems. As with the chlorinated hydrocarbons and methyl orange, we noticed an inverse correlation between phenol's initial rate constant for and the initial concentration as shown in Figure 9. This inverse relationship between degradation rates and initial solute concentrations is consistent with previous findings^{8,21,39} and indicates significant scavenging of free-radical species by the in-situ degradation by-products.

Effect of Reactor Flow on Degradation Rates

In an effort to evaluate and optimize the performance of the Pilotstation reactor, we also investigated what effect flow rate through the Pilotstation had on reaction kinetics. In addition to the previous experiments performed at $F = 6$ L/min, the degradation kinetics of DCM, MO, and phenol were measured at $F = 1.5, 4, 9$ and 12 L/min. ($[DCM]_0 = 2500$ μ M, $[MO]_0 = 10$ μ M, $[phenol]_0 = 670$ μ M) Rate constants measured at each flow rate, k_F , were normalized to the rate constant at $F = 6$ L/min (i.e., $k_{norm} = k_F/k_6$). These normalized rates are plotted vs. flow rate in Figure 10. Normalized rates varied by 10% and 20% for MO and DCM, respectively. No discernable trends related to flow rate were found for the degradation of these two compounds. Phenol, on the other hand, was found to be quite sensitive to conditions within the reactor, with degradation rates deviating by more than 50% as flow was varied about $F = 6$ L/min.

The differences observed for these solutes can be attributed most likely to effects related to the distribution of these species within the solution undergoing sonolysis. As mentioned previously, DCM readily diffuses into cavitation bubbles where it is subsequently degraded during cavitation bubble implosion. MO and phenol are non-volatile compounds and are limited to free-radical reactions within the bulk solution. However, the aqueous solubility of DCM is nearly 80-fold smaller than that of phenol (8.3 g/100 mL – MSDS EM Science), suggesting that DCM will be in excess at the cavitation bubble interface where the local concentration of $\cdot\text{OH}$ is higher, while phenol will reside in the bulk solution. These preliminary results suggest that reactions operating within the bubble or in the solution near the bubble interface are not appreciably affected by changes in the flow rate through the reactor, but reactions occurring in the bulk solution are more sensitive to this parameter.

Evaluation of $\cdot\text{OH}$ radical production

Considering the varying response observed in the three studied reactors, an estimation of the available concentration of $\cdot\text{OH}$ radicals can be made in each case, assuming that a steady state concentration $[\cdot\text{OH}]_{\text{ss}}$ exists inside the reaction vessel during sonolysis. The short lifetime of $\cdot\text{OH}$ radicals makes it virtually impossible for them to exist outside the reactor vessel in flow systems, at the present circulation rates. The steady state $\cdot\text{OH}$ concentration, $[\cdot\text{OH}]_{\text{ss}}$, is included in the expression of the MO degradation rate, as follows:

$$d[\text{MO}] / d t = k_{\cdot\text{MO}}^{\text{OH}} [\cdot\text{OH}]_{\text{ss}} [\text{MO}] \quad (8)$$

and therefore it can be calculated from the value of the measured pseudo first-order rate constant, k_{-MO} , and the reported value⁴⁰ for the bimolecular rate constant $k_{-MO}^{OH} = 2 \times 10^{10} \text{ M}^{-1}\text{s}^{-1}$, as

$$[\cdot\text{OH}]_{ss} = k_{-MO} / k_{-MO}^{OH} \quad (9)$$

In the case of the two small-scale reactors, $[\cdot\text{OH}]_{ss}$ can be calculated with the values of k_{-MO} determined in the absence of external circulation (see Table 1). Due to heat dissipation limitations, the Pilotstation can not be operated without flowing through the external heat exchanger. Therefore, it is not possible to measure directly the rate constant corresponding to a total operation volume equivalent to only that of the reactor vessel ($V_V = 6 \text{ L}$). We define the rate constant k_{-MO}^* for the degradation of MO in the Pilotstation. Assuming ideal CSTR-behavior and neglecting temperature effects, the mass balance equations within the heat exchanger and in the ultrasonic vessel are given as^{41,42}

$$\frac{d[\text{MO}]_{HE}(t)}{dt} = \frac{F}{(V_T - V_V)} ([\text{MO}]_V(t) - [\text{MO}]_{HE}(t)) \quad (10)$$

$$\frac{d[\text{MO}]_V(t)}{dt} = \frac{F}{V_V} ([\text{MO}]_{HE}(t) - [\text{MO}]_V(t)) - k_{-MO}^* [\text{MO}]_V(t) \quad (11)$$

where $[\text{MO}]_V(t)$ and $[\text{MO}]_{HE}(t)$ are the concentration of substrate in the vessel and the heat exchanger, respectively, F is the flow rate (in this case, 6 L/min) and V_T is the total

volume of solution treated (i.e., the combined volumes of the reaction chamber, the tubing and the reservoir). At $t = 0$, $[MO]_V(t) = [MO]_{HE}(t) = [MO]_0$. Solving equations 10 and 11⁴², the rate constant k_{-MO}^* corresponding to the sonochemical reaction in the vessel can be related with the observed overall rate constants k_{-MO} for different total volumes reported in Table 1 and Figure 8, as

$$k_{-MO} = \left(\frac{V_V}{V_T} \right) k_{-MO}^* \quad (12)$$

By combining Equation 7 and 12, we estimated $k_{-MO}^* = 0.103 \text{ min}^{-1}$, which permitted us to calculate $[\cdot OH]_{ss}$ inside the reaction vessel of our Pilotstation, according to equation 9. That value, together with those calculated for the small reactors, is reported in Table 3. The Pilotstation produces the highest $\cdot OH$ radical steady-state concentration, however that chemical response is not necessarily linear with the power density, reflecting other effects intrinsic to the specific reactor design.

Power budget analysis

The main technical problem to be overcome in further scale-up of sonochemical reactors is related with heat dissipation. High-frequency transducers operating in the kW range must be constantly chilled in order to prevent their inactivation. The use of PTFE windows improves the operation of the system at higher applied powers. These thin windows do not interfere with the propagation of the acoustic field, but are able to separate the treated solution inside the Pilotstation from the heat-transfer fluid cooling the

transducer surface. Instead of employing the treated solution as a main heat sink, in this configuration most of the heat produced by the transducers is directly absorbed by a relatively small amount of cooling fluid in contact with their surface, which is controlled by an independent thermostat. Thus, the working temperature of the solution under irradiation may vary within a range, and can be adjusted by changing the operation conditions on the heat exchanger unit. This important design improvement makes the Pilotstation a very flexible unit in on-line flow systems, where the temperature of the fluid depends on other parameters of the process, and might not be completely controlled during the transit through the sonochemical reactor.

A power budget can be estimated for the operation of our Pilotstation; this provides a useful tool to assess the efficiency of transforming electrical power to sonochemical activity.⁴³ The power consumption can be described as shown in the flow diagram of Figure 11. The total power output of the transducers (P) is converted into acoustic power transmitted to the vessel (P_{US}) and heat directly dissipated at the transducers' surface per unit time (Q_{TS}), as follows:

$$P = P_{US} + Q_{TS} \quad (13)$$

The acoustic power reaching the vessel, P_{US} , is then utilized in cavitation events with the consequent chemical processes associated with them (W_{US}), all of which are accompanied by further heat production within the reaction vessel (Q_{US}):

$$P_{US} = W_{US} + Q_{US} \quad (14)$$

We have evaluated the heat production and consumption in each stage through conventional calorimetric methods. In the case of the heat dissipated at the transducers' surface, a mass $M_T = 36$ kg of cooling water initially at 3.0 °C was circulated through the

cooling jackets at the same flow rate used during regular operation of the Pilotstation. Temperature changes, dT/dt , were recorded with and without operating the transducers, allowing for an evaluation of Q_{TS} as follows:

$$Q_{TS} = M_T \cdot Cp \left(\frac{dT}{dt} \right) \quad (15)$$

where Cp is the specific heat of the solution ($4.18 \text{ J g}^{-1} \text{ K}^{-1}$). This estimation yielded a value of $Q_{TS} = 880 \text{ W}$.

Similarly, temperature profiles represented in Figure 3 were used to estimate the amount of heat produced during bubble cavitation inside the reaction vessel. The change in temperature as a function of time during sonolysis, (dT/dt) , was numerically evaluated over the temperature range $3\text{--}9 \text{ }^\circ\text{C}$ from the initial slope of the average of T_1 and T_2 . In this case, however, the heat dissipated at the heat exchanger (Q_{HE}) and at the PTFE windows (Q_{PTFE}) must also be taken into consideration

$$Q_{US} = M_V \cdot Cp \left(\frac{dT}{dt} \right) + Q_{HE} + Q_{PTFE} \quad (16)$$

($M_V = 7.25 \text{ kg}$ is the mass of treated solution). The latter two values in equation 16 were also determined calorimetrically, in the absence of ultrasonic irradiation, over the same temperature interval. These independent determinations resulted in the values $Q_{HE} = 215 \text{ W}$ and $Q_{PTFE} < 10 \text{ W}$. Heat gains from the surrounding atmosphere can be neglected, considering this last value. By this procedure we estimated that not less than $Q_{US} = 970 \text{ W}$ are actually degraded mechanically during cavitation resulting in heat production inside the reaction vessel, which represents nearly a third of the total power input. Therefore, the actual power consumed by cavitation and sonochemical processes is $W_{US} = 1150 \text{ W}$. This value is approximately one third of the total power input to the system.

Comparison with other advanced oxidation technologies

Comparisons of power density utilization between sonochemical methods and photocatalytic techniques, as applied to the same chemical systems, provide a relative estimation of the energy efficiency of ultrasonic irradiation. The normalized parameter

$$\xi = \frac{\text{initial reaction rate}}{\text{power density}} \left(\frac{mM / hour}{W / L} \right) \quad (17)$$

permits us to compare data from different experiments. We observed in all cases an important improvement of efficiency (i.e., higher ξ values) when ultrasonic irradiation is employed. At high frequencies (in the range 100-1000 kHz) ξ is maximized, reaching a difference up to two orders of magnitude as compared with values for photocatalysis. Table 4, 5 and 6 contain the data for a variety of degradation substrates, namely the non-ionic surfactant Triton X-100 (Table 4), the volatile chlorinated hydrocarbons CCl₄ and CHCl₃ (Table 5) and the aromatic compound 4-chlorophenol (Table 6). This data illustrates the potential of sonochemistry as a useful advanced oxidation process.

Conclusions

The UES 4000-C Pilotstation ultrasound reactor is demonstrated to be an effective system for the oxidation of both volatile and non-volatile organic solutes within aqueous solutions. Solution volume was varied between 7.25 and 45 L with no appreciable loss in the sonochemical efficiency of the system. The main technical problems to be overcome in further scale-up of sonochemical reactors are related with heat dissipation. High frequency transducers operating in the kW range must be constantly chilled in order to prevent their inactivation. The use of PTFE windows improves the operation of the

system at higher applied powers. These thin windows do not interfere with the propagation of the acoustic field, but are able to separate the treated solution inside the Pilotstation from the heat-transferring fluid cooling the transducer surface. Instead of employing the treated solution as a main heat sink, in this configuration most of the waste heat produced by the transducers is absorbed by a relatively small amount of cooling fluid, which is controlled by an independent thermostat. Thus, the working temperature of the solution might vary within a range, and can be adjusted by changing the operation conditions at the heat exchanger unit. This important design improvement makes the Pilotstation a potentially very flexible unit in on-line flow systems, where the temperature of the fluid depends on other parameters of the process, and might not be completely controlled during the transit through the sonochemical reactor.

Acknowledgement

The authors thank Thomas W. Alderson II for his collaboration during the initial steps of this work. Financial support provided by the Department of Energy (DOE 1963472402) and the U.S. Navy (N 47408-99-M-5049) is gratefully acknowledged.

References

- (1) Mason, T. J.; Lorimer, J. P. *Sonochemistry. Theory, Applications and Uses of Ultrasound in Chemistry*; Wiley: New York, 1988.
- (2) Mason, T.; Lorimer, J. *Applied Sonochemistry. The Uses of Power Ultrasound in Chemistry and Processing*; Wiley-VCH: Weinheim, Germany, 2002.
- (3) Leighton, T. G. *The Acoustic Bubble*; Academic Press: London, 1994.
- (4) Thompson, L.; Doraiswamy, L. *Ind. Eng. Chem. Res.* **1999**, *38*, 1215.
- (5) Martin, P.; Ward, L. *Chem. Eng. Res. Des.* **1992**, *70*, 296.
- (6) Harwell. *Chem. Eng.* **1990**, *23*, 15.
- (7) Hua, I.; Hoffmann, M. *Environ. Sci. Technol.* **1997**, *31*, 2237.
- (8) Petrier, C. *J. Phys. Chem.* **1994**, *98*, 10514.
- (9) Petrier, C.; Francony, A. *Ultrasonics Sonochemistry* **1997**, *4*, 295.
- (10) Beckett, M.; Hua, I. *J. Phys. Chem. A* **2001**, *105*, 3796.
- (11) Hua, I.; Hoffmann, M. *Environ. Sci. Technol.* **1996**, *30*, 864.
- (12) Hung, H.; Hoffmann, M. *J. Phys. Chem. A* **1999**, *103*, 2734.
- (13) Weavers, L.; Ling, F.; Hoffmann, M. *Environ. Sci. Technol.* **1998**, *32*, 2727.
- (14) Weavers, L.; Malmstadt, N.; Hoffmann, M. *Environ. Sci. Technol.* **2000**, *34*, 1280.
- (15) Destailats, H.; Hung, H.; Hoffmann, M. *Environ. Sci. Technol.* **2000**, *34*, 311.
- (16) Joseph, J.; Destailats, H.; Hung, H.; Hoffmann, M. *J. Phys. Chem. A* **2000**, *104*, 301.
- (17) Destailats, H.; Colussi, A. J.; Joseph, J. M.; Hoffmann, M. R. *J. Phys. Chem. A* **2000**, *104*, 8930.

- (18) Destailats, H.; Alderson II, T. W.; Hoffmann, M. R. *Environ. Sci. Technol.* **2001**, *35*, 3019.
- (19) Naffrechoux, E.; Chanoux, S.; Petrier, C.; Suptil, J. *Ultrasonics Sonochemistry* **2000**, *7*, 255.
- (20) Peller, J.; Wiest, O.; Kamat, P. *J. Phys. Chem. A* **2001**, *105*, 3176.
- (21) Rong, L.; Yasuda, K.; Bando, Y.; Nakamura, M. *Jpn. J. Appl. Phys.* **2002**, *41*, 3272.
- (22) Vinodgopal, K.; Peller, J. *Res. Chem. Intermediat* **2003**, *29*, 307.
- (23) Tezcanli-Guyer, G.; Ince, N. *Ultrasonics Sonochemistry* **2003**, *10*, 235.
- (24) Colussi, A.; Weavers, L.; Hoffmann, M. *J. Phys. Chem. A* **1998**, *102*, 6927.
- (25) Suslick, K. S.; Mdleleni, M. M.; Ries, J. T. *J. Am. Chem. Soc.* **1997**, *119*, 9303.
- (26) Colussi, A.; Hoffmann, M. *J. Phys. Chem. A* **1999**, *103*, 2696.
- (27) Storey, B.; Szeri, A. *Proc. R. Soc. London, Ser. A* **2000**, *456*, 1685.
- (28) Storey, B.; Szeri, A. *Proc. R. Soc. London, Ser. A* **2001**, *457*, 1685.
- (29) Szeri, A.; Storey, B.; Pearson, A.; Blake, J. *Phys. Fluids* **2003**, *15*, 2576.
- (30) Yasui, K. *J. Phys. Soc. Jpn.* **1997**, *66*, 2911.
- (31) Yasui, K. *J. Chem. Phys.* **2001**, *115*, 2893.
- (32) Yasui, K.; Tuziuti, T.; Iida, Y.; Mitome, H. *J. Chem. Phys.* **2003**, *119*, 346.
- (33) Kang, J.; Hung, H.; Lin, A.; Hoffmann, M. *Environ. Sci. Technol.* **1999**, *33*, 3199.
- (34) Berlan, J.; Trabelsi, F.; Delmas, H.; Wilhelm, A.; Pettrignani, J. *Ultrasonics Sonochemistry I* **1994**, 1994.
- (35) Lide D. R., e. *Handbook of Chemistry & Physics*; CRC: Boca Raton, 1998.
- (36) Colussi, A.; Hung, H.; Hoffmann, M. *J. Phys. Chem. A* **1999**, *103*, 2696.

- (37) Choi, W.; Hoffmann, M. *Environ. Sci. Technol.* **1997**, *31*, 89.
- (38) Schwarzenbach, R.; Gschwend, P.; Imboden, D. *Environmental Organic Chemistry*, 1st ed.; John Wiley and Sons: New York, 1993.
- (39) Kotronarou, A.; Mills, G.; Hoffmann, M. *J. Phys. Chem.* **1991**, *95*, 3630.
- (40) Buxton, G.; Greenstock, C.; Helman, W.; Ross, A. *J. Phys. Chem. Ref. Data* **1988**, *17*, 513.
- (41) Aris, R. *Elementary Chemical Reactor Analysis*; Prentice-Hall Inc.: Englewood Cliffs, NJ, 1969.
- (42) Hua, I.; Hochemer, R.; Hoffmann, M. *Environ. Sci. Technol.* **1995**, *29*, 2790.
- (43) Kotronarou, A.; Mills, G.; Hoffmann, M. *Environ. Sci. Technol.* **1992**, *26*, 2420.
- (44) Pelizzetti, E.; Minero, C.; Maurino, V.; Sciafani, A.; Hidaka, H.; Serpone, N. *Environ. Sci. Technol.* **1989**, *23*, 1380.
- (45) Brand, N.; Mailhot, G.; Bolte, M. *Environ. Sci. Technol.* **1998**, *32*, 398.
- (46) Peill, N.; Hoffmann, M. *Environ. Sci. Technol.* **1998**, *32*, 398.

Table 1: Summary of experimental conditions for DCM, TCE and MO, and observed pseudo first-order rate constant (k_{-X}) and half-life time ($t_{1/2}$) in air-saturated solutions.

Reactor	Power W/L	Init. Conc. μM	Flow rate L/min	Vol. L	$k_{-X} * 10^3$ Min^{-1}	$t_{1/2}$ min
DCM						
Allied Signal	83	177	0	0.6	16.2	42.7
Allied Signal	166	1495	0	0.6	50.6	13.7
UES-4000 C	414	2543	6	7.25	91.4	7.6
UES-4000 C	414	1177	6	7.25	133.8	5.2
TCE						
Undatim	77	1408	0	0.65	33	21.0
Undatim	77	251	0	0.65	45	15.4
Undatim	77	38	0	0.65	50	13.9
UES-4000 C	414	107	6	7.25	203	3.4
UES-4000 C	414	571	6	7.25	163	4.3
MO						
Allied Signal	50	10	2.4	2	5.53	125.3
Allied Signal	166	10	0	0.6	19.76	35.1
Undatim *	93	10	0	0.65	42	16.5
UES-4000 C	67	10	6	45	15	46.2
UES-4000 C	150	10	6	20	29.5	23.5
UES-4000 C	214	10	6	14	46.6	14.9
UES-4000 C	300	10	6	10	58	11.9
UES-4000 C	353	10	6	8.5	71	9.8
UES-4000 C	414	10	6	7.25	88.5	7.8

* not measured in this work, see ref. 17

Table 2: Summary of experimental conditions for Phenol, and normalized initial rate constant (k_{-Ph}/C_0) in air-saturated solutions.

Reactor	Power density W/L	Init. Conc. μM (C_0)	Flow rate L/min	Volume L	$(k_{-Ph}/C_0) * 10^3$ min^{-1}
Allied Signal	166	64	0	0.6	29.3
Allied Signal	166	617	0	0.6	6.2
Allied Signal	166	819	0	0.6	6.3
Allied Signal	166	6,096	0	0.6	1.1
UES-4000 C	414	53	6	7.25	63.0
UES-4000 C	414	670	6	7.25	30.1
UES-4000 C	414	6165	6	7.25	2.7

Table 3: Steady-state $\cdot\text{OH}$ radical concentration determined for each reactor.

Reactor	$[\cdot\text{OH}]_{ss} \times 10^{-14}$ (M)
Pilotstation	8.58×10^{-14}
Undatim	3.50×10^{-14}
Allied Signal	1.65×10^{-14}

Table 4: Comparison of energy efficiency between ultrasonic degradation (US) and photocatalysis (PC) in the case of the non-ionic surfactant Triton X-100.

Method	Power	Vol.	Power density	Triton X-100 concentration	Observed Rate constant	Half-life time	Initial reaction rate	Method efficiency (reaction rate / power density)
Units	W	L	W/L	mM	min ⁻¹	min	mM/hour	(mM/hr) / (W/L) × 10 ⁵
US @ 250 kHz (ref 15)	4000	20	200	0.03 to 1.13	21.5 to 0.7	32 to 990	0.05 to 0.1	25 to 50
PC (in TiO ₂ suspensions) (ref 44)	1500	0.03	47,700	0.21	0.2	3.5	2.4	5
PC in H ₂ O (ref 45)	125	0.06	2,100	0.46	0.003	220	0.084	4

Table 5: Comparison of energy efficiency between ultrasonic degradation (US) and photocatalysis (PC) in the case of chlorinated methanes.

A) CCl₄

Method	Power	Vol.	Power density	CCl₄ Conc.	Observed Rate constant	Half-life time	Initial reaction rate	Method efficiency (reaction rate / power density)
Units	W	L	W/L	mM	min ⁻¹	min	mM/hour	[(mM/hr) / (W/L)] × 10 ⁵
US @ 20 kHz (ref 12)	62	0.095	650	0.2	0.025	28	0.30	46
US @ 205 kHz (ref 12)	35	0.60	58	0.2	0.044	16	0.53	914
PC (TiO ₂ susp.)(ref 37)	910	0.035	26000	5			2.5	9.6

B) CHCl₃

Method	Power	Vol.	Power density	CHCl₃ Conc.	Observed Rate constant	Half-life time	Initial reaction rate	Method efficiency (reaction rate / power density)
Units	W	L	W/L	MM	min ⁻¹	min	mM/hour	(mM/hour) / (W/L) × 10 ⁵
US @ 205 kHz (ref 12)	35	0.60	58	0.2	0.028	25	0.34	586
PC (TiO ₂ susp.)(ref 37)	910	0.035	26000	63			0.72	2.7

Table 6: Comparison of energy efficiency between ultrasonic degradation (US) and photocatalysis (PC) in the case of 4-chlorophenol (4-CP).

Method	Power	Vol.	Power density	4-CP Init.conc.	Observed Rate constant	Half-life Time	Initial reaction rate	Method efficiency (reaction rate / power density)
Units	W	L	W/L	mM	min ⁻¹	min	mM/hour	(mM/hour)/(W/L) × 10 ⁵
SC @ 20 kHz (ref 13)	56	0.24	233	0.1	0.0017	407	0.01	4.3
SC @ 500 kHz (ref 13)	48	0.64	75	0.1	0.021	33	0.13	173
PC (TiO ₂ susp.)(ref 46)	1000	0.19	5200	0.1			0.08	1.5

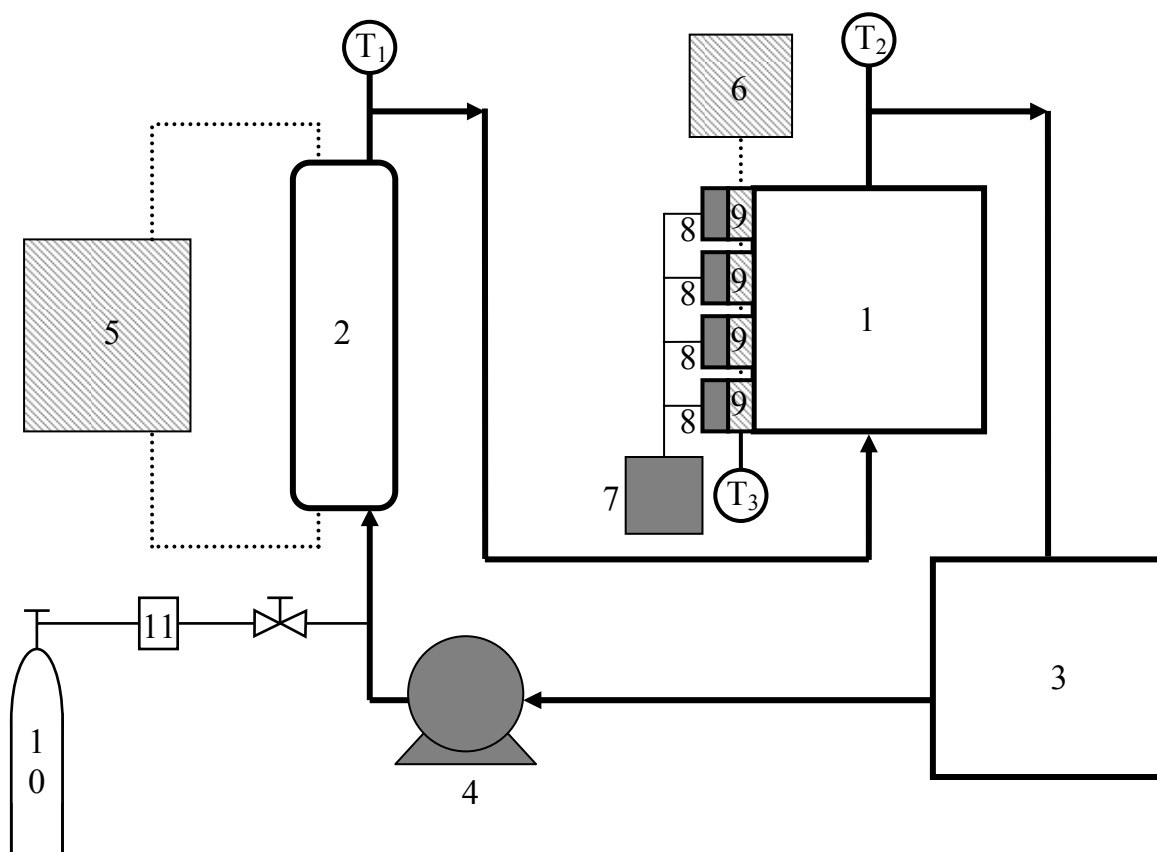


Figure 1. Experimental setup. 1: reaction vessel; 2: heat exchanger; 3: recirculating tank; 4: peristaltic pump; 5: chiller; 6: thermostat; 7: sonochemical power supply; 8: piezoelectric transducers; 9: transducers cooling jacket; 10: background gas supply; 11: flow meter; T_1 : thermometer at the exit of the heat exchanger; T_2 : thermometer at the exit of the ultrasonic vessel; T_3 : thermometer at the transducer cooling jacket.

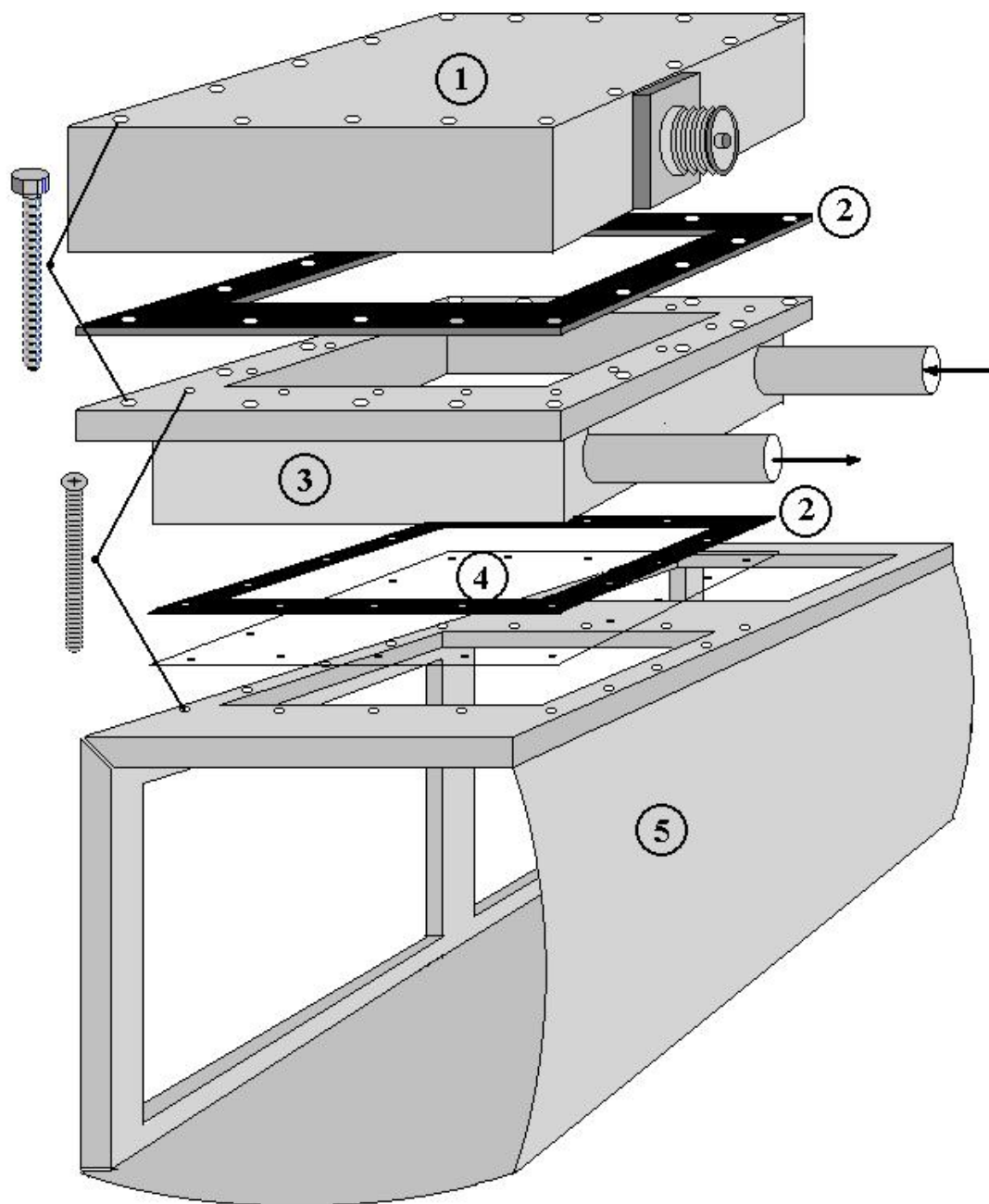


Figure 2: Pilotstation reactor vessel. 1: transducer housing (17.5 cm x 17.5 cm); 2: gasket; 3: transducer cooling water jacket; 4: PTFE acoustic window (11.5 cm x 11.5 cm); 5: reactor vessel body. Vessel is shown with one of four transducers, and with end-closures removed.

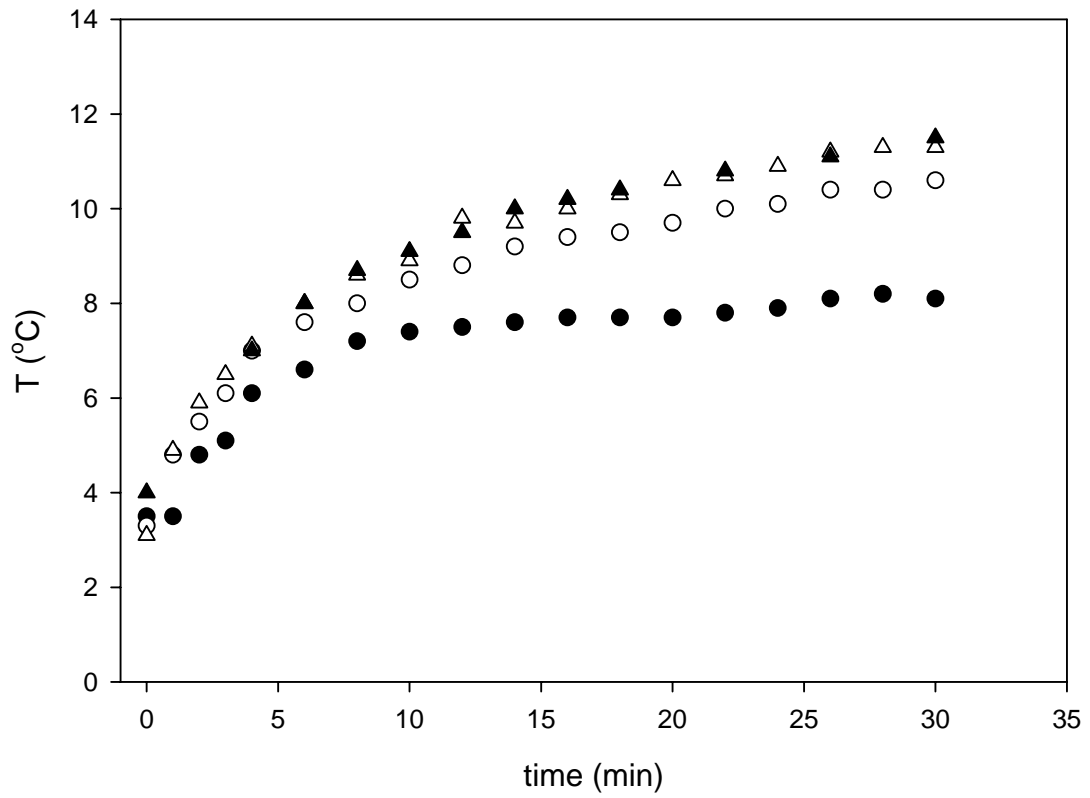


Figure 3: Temperature profiles leaving the heat exchanger (T_1) during a 30-minute run in the UES 4000C Pilotstation as a function of flow rate (L min^{-1}). ●: 1.5; ○: 4.0; △: 9.0; ▲: 12.0.

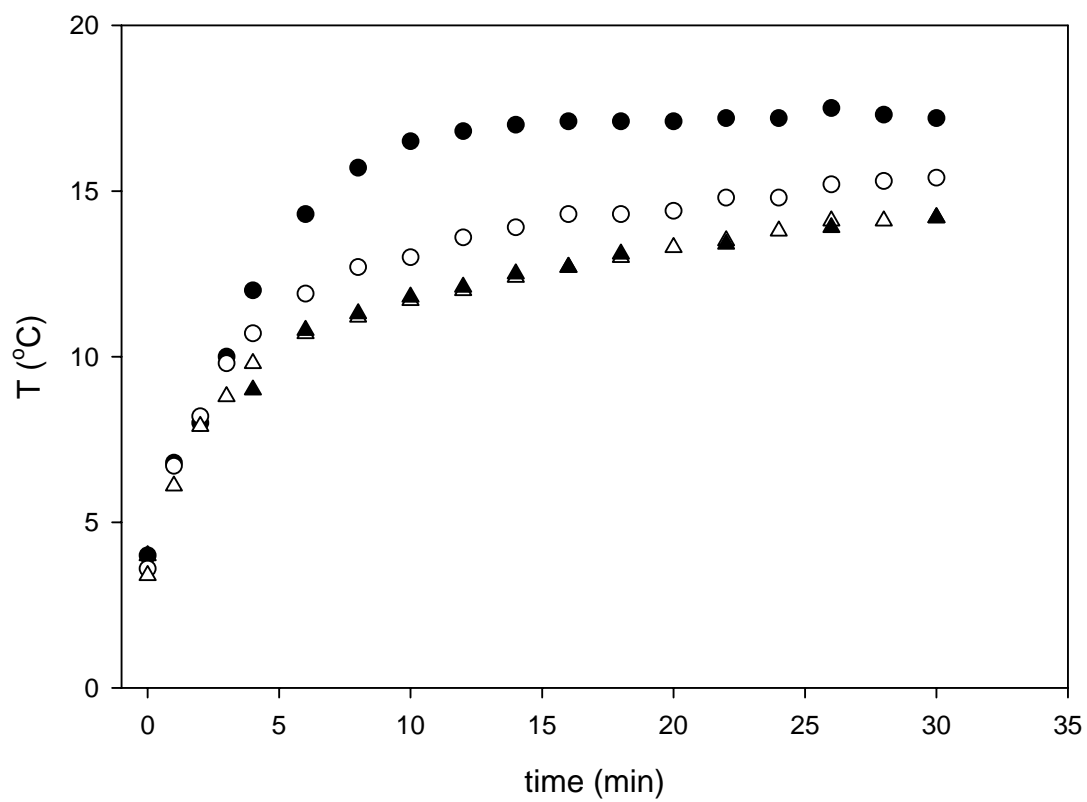


Figure 4: Temperature profiles leaving the ultrasonic vessel (T_2) during a 30-minute run in the UES 4000C Pilotstation as a function of flow rate (L min^{-1}). ●: 1.5; ○: 4.0; △: 9.0; ▲: 12.0.

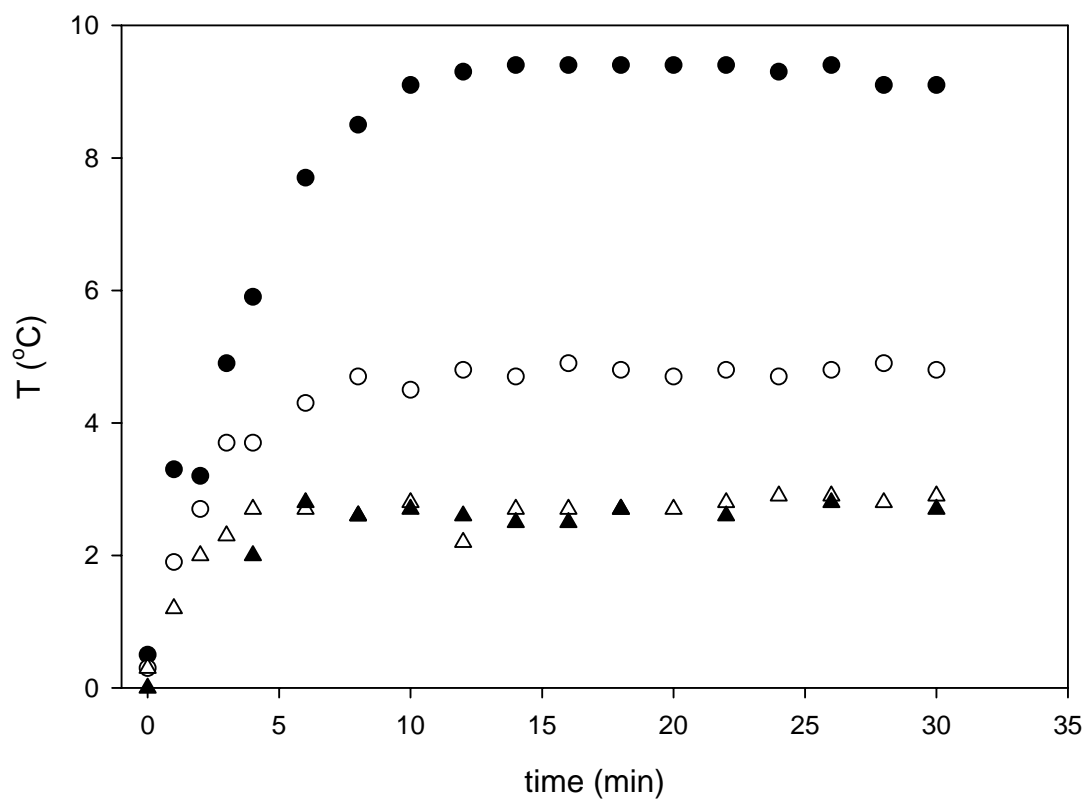


Figure 5: Temperature gradient across the ultrasonic vessel (T_2-T_1) during a 30-minute run in the UES 4000C Pilotstation as a function of flow rate ($L\ min^{-1}$). ●: 1.5; ○: 4.0; △: 9.0; ▲: 12.0

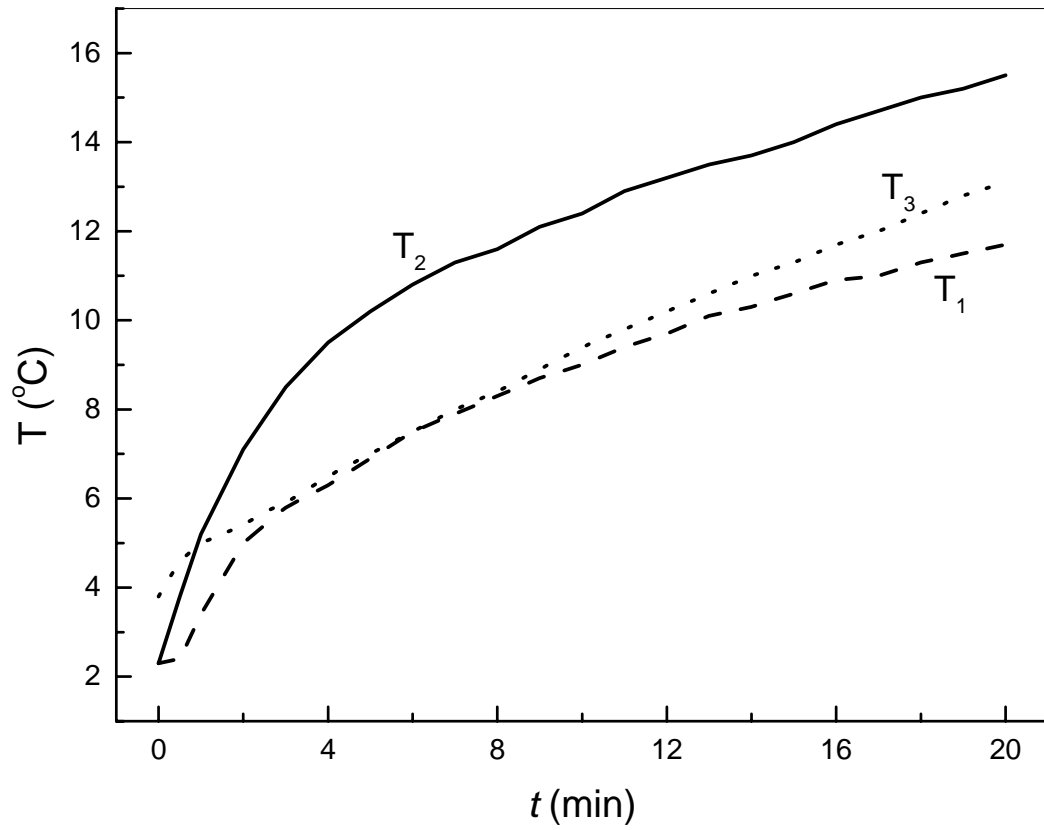


Figure 6: UES Pilotstation temperature profiles during a 20-minute run in the UES 4000C Pilotstation : Solution exiting the ultrasonic vessel, T_2 (solid line), exiting the heat exchanger, T_1 (dashed line) and temperature in the transducers cooling jacket, T_3 (dotted line)

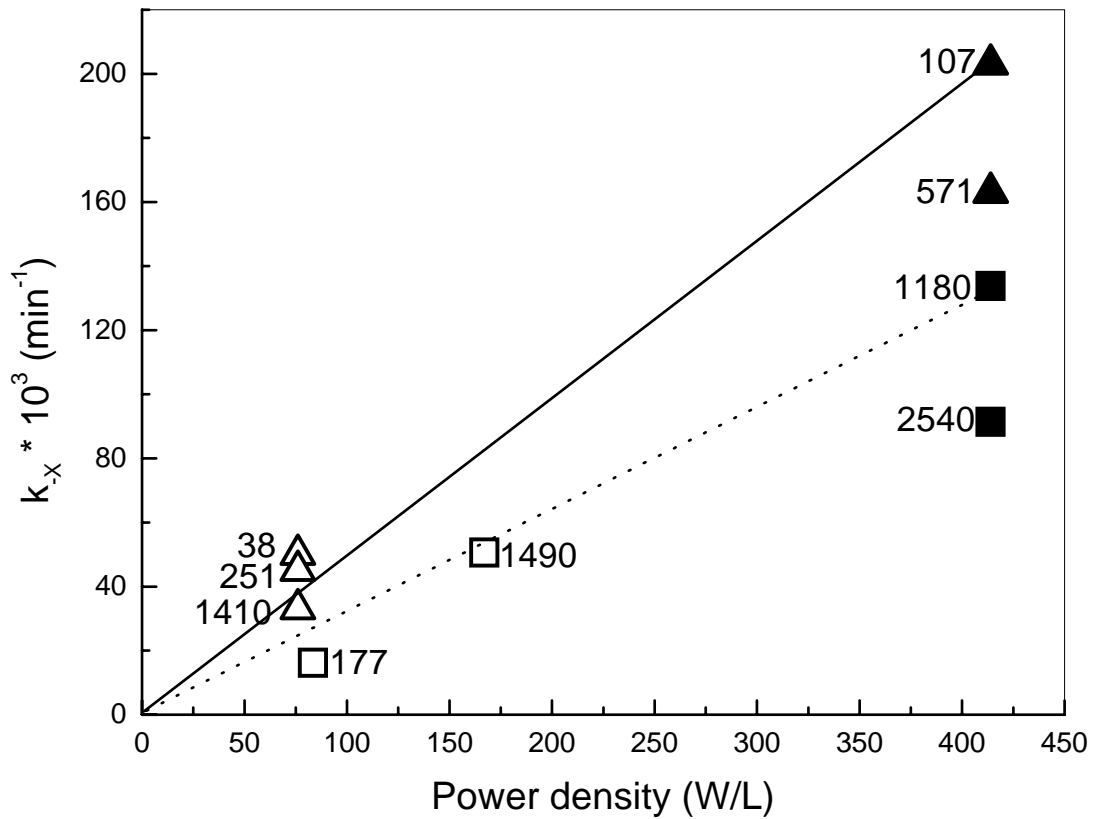


Figure 7: Pseudo-first order sonochemical degradation rate constant of chlorinated volatile substrates. **▲**: TCE in Pilotstation; **△**: TCE in Undatim bench-scale reactor; **■**: DCM in Pilotstation; **□**: DCM in Allied Signal bench-scale reactor. The concentration (in μM) is indicated for each data point. The solid and dotted lines represent the expected linear behavior with respect to the power density for the lowest concentrations of TCE and DCM in the Pilotstation, respectively.

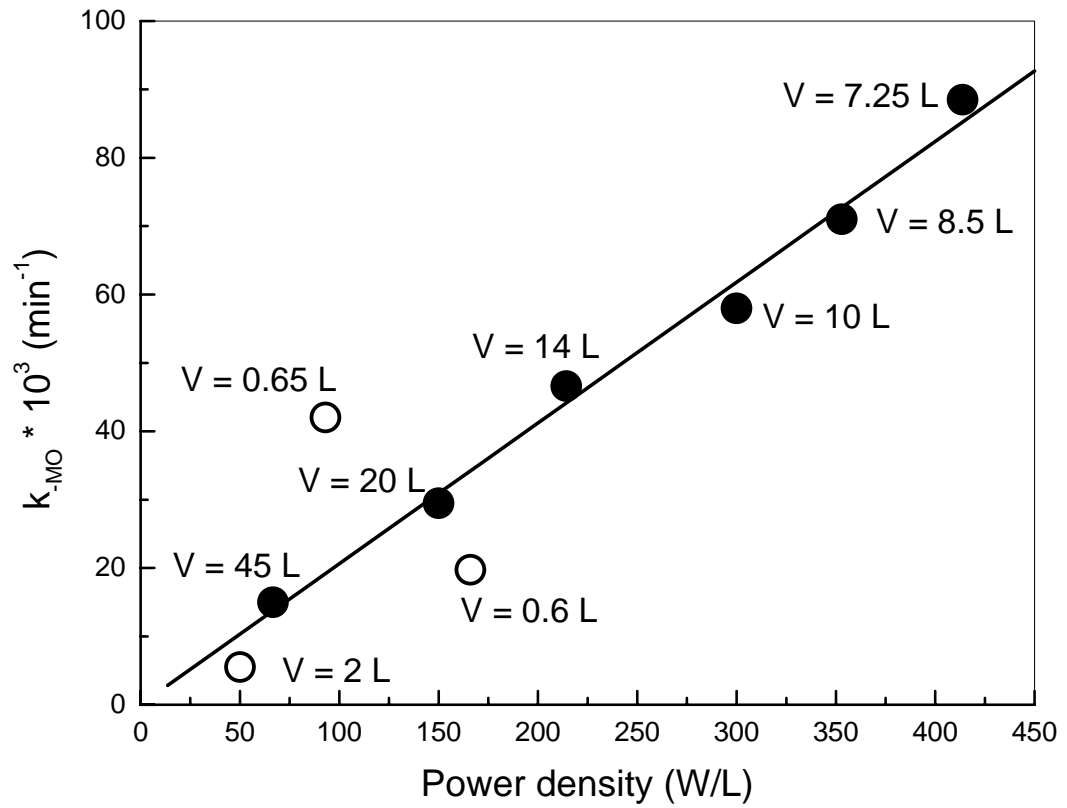


Figure 8: Pseudo-first order sonochemical degradation rate constant of 10 μM MO (aq).
● Pilotstation; O: bench-scale reactors.

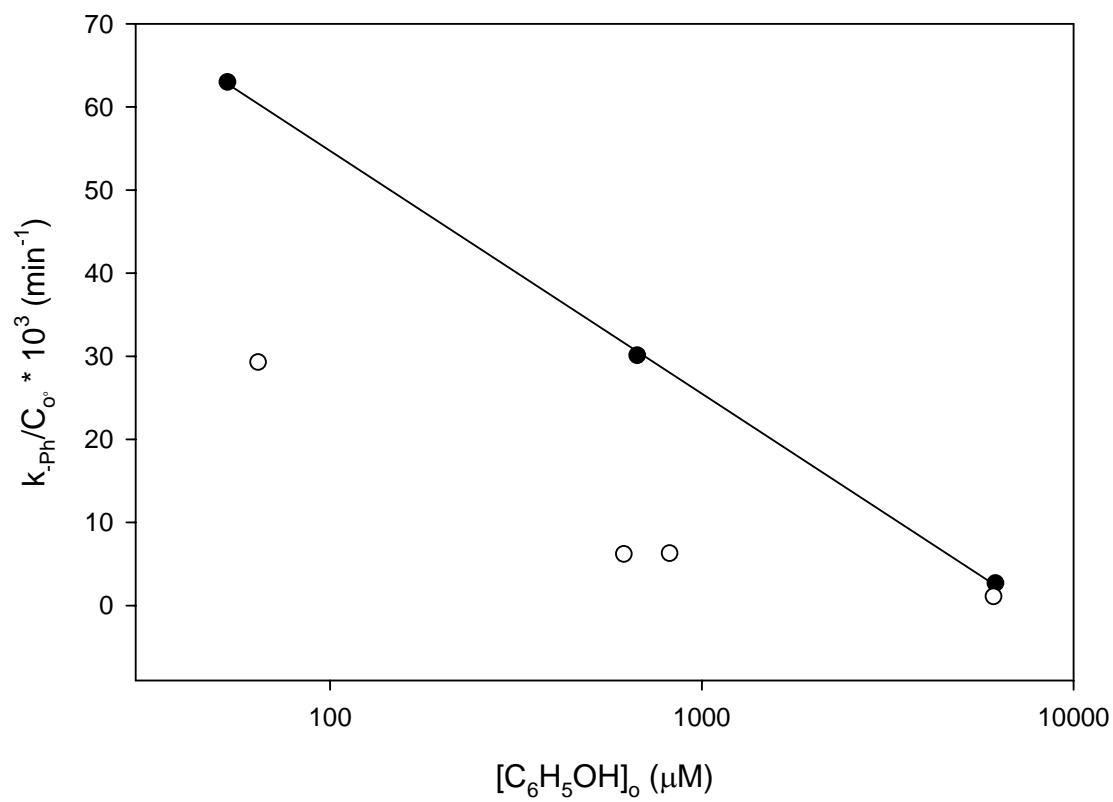


Figure 9: Normalized initial sonochemical degradation rate for phenol.
● Pilotstation; ○ bench-scale reactors.

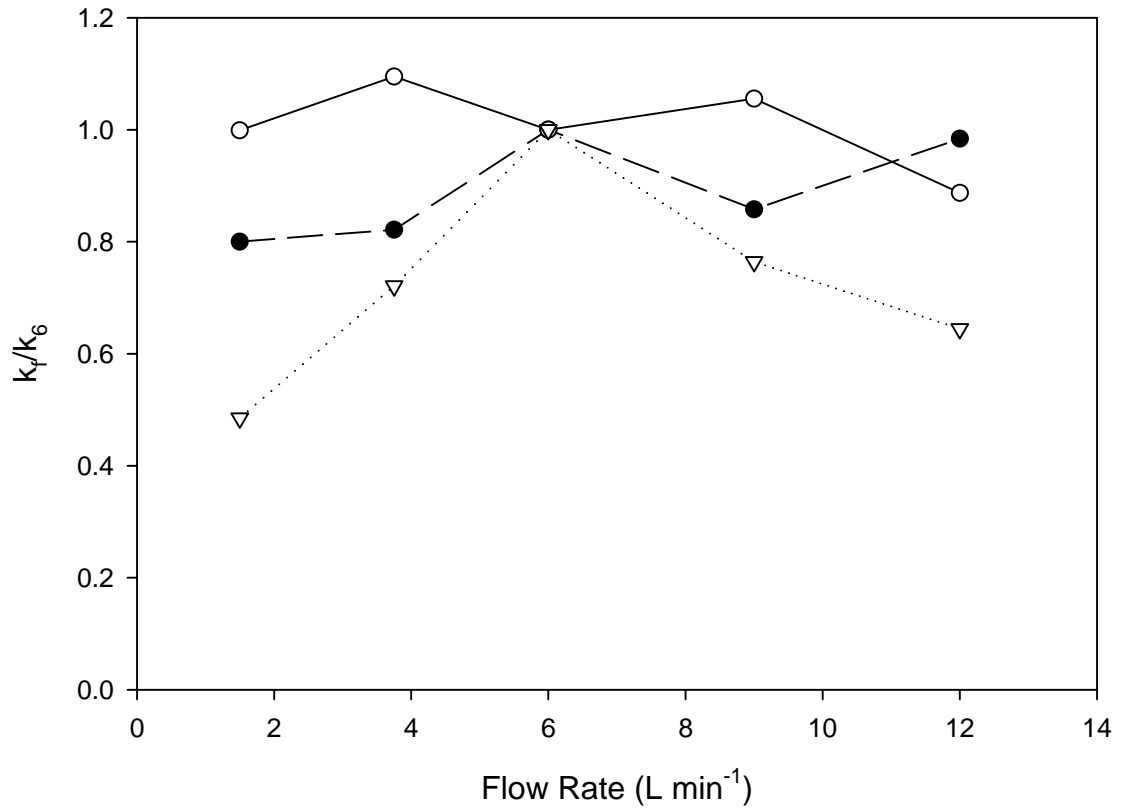


Figure 10: Normalized degradation rates run in the UES 4000C Pilotstation as a function of flow rate (L min⁻¹). ●: DCM; ○: MO; ▽: Phenol.

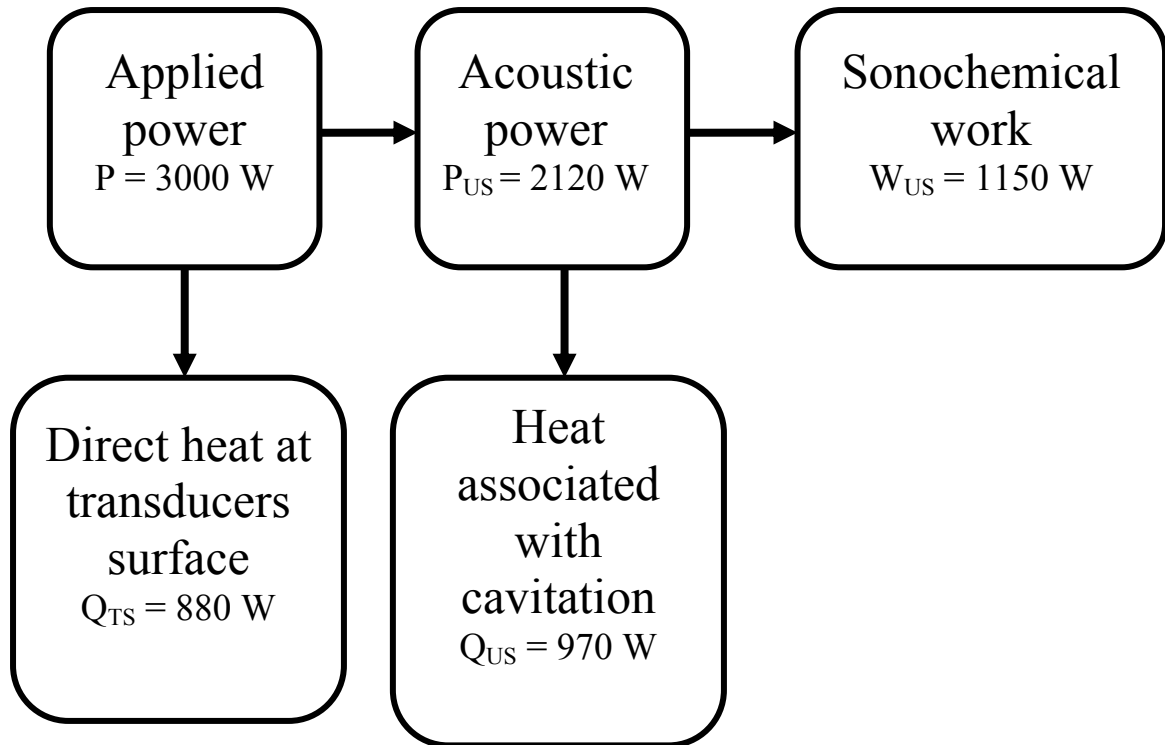


Figure 11. Power budget analysis for the Pilotstation.